PHYSICAL REVIEW B VOLUME 24, NUMBER 8 15 OCTOBER 1981

Multiple-scattering effects in ion-surface interactions at low energies

D. P. Jackson
Atomic Energy of Canada Limited Research Company, Chalk River, Ontario KOJ 1J0, Canada

W. Heiland
University of Osnabrück, Postfach 4469, 45 Osnabrück, Germany

E. Taglauer
Max Planck Institute for Plasmaphysics, EURATOM Association, D-8046 Garching bei München, Germany

(Received 26 March 1981)

The scattering of 600-eV He ions from clean Ni(110) is studied both experimentally and by means of computer simulation. It is shown that for a comparison with the experimental data it is essential that the scattering model be three dimensional. We infer from such comparisons for the dependence of the ion yields on the crystallographic orientation that neutralization effects are operating which strongly depend on the scattered particles' trajectories. Two types of neutralization processes are distinguished: one essentially Auger and the other more typical of the bulk neutralization seen at higher energies.

I. INTRODUCTION

In a previous Letter[1] we reported strong evidence for trajectory-dependent neutralization effects in the scattering of low-energy He^+ and Li^+ ions from a clean Ni(110) surface. The interpretation of these effects depends in turn on the comparison of experimental data with the computer code ARGUS in order to elucidate the multiple-scattering processes involved in determining the scattered particle spectra. In this paper we shall discuss the details of these processes and their influence on neutralization for 600-eV He^+ ions incident on a clean Ni(110) surface for which extensive experimental data is available.

Multiple-scattering effects have been studied in the past mainly with heavier ions (Ne^+, Ar^+) over a wide energy range.[2] First interpretations followed the principal idea of Parilis,[3] i.e., the effects are due to sequences of single binary collisions, in the simplest case double collisions. These efforts lead to the development of "chain" or "string" models for multiple scattering, from which one could evaluate some properties of scattering effects, i.e., mass-ratio dependence, energy dependence, angular dependences, etc., at least qualitatively. These models fail, however, when quantitative intensities of scattered fluxes are to be evaluated. It has been shown that better agreement with experiment can be achieved by using a fully three-dimensional program,[4] taking into account thermal vibrations and slight adjustments of the interaction potentials involved. For light-ion backscattering, however, the program used, MARLOWE,[5] requires excessive computer time to obtain statistically valid results. Similarly the recent calculations of Garrison[6] illustrate the essential features but also suffer from statistical difficulties in interpretation. Nevertheless a detailed analysis of the elastic interaction between ions and solids is needed for an understanding of the whole phenomenon, which is in large measure dominated by neutralization effects.[7] In the case of He^+ on polycrystalline Ni, experiments gave evidence[8,9] that the neutralization is due to an Auger neutralization process, i.e., the probability for the ions to survive the surface collision is

$$P=\exp(-v_0/v)\,, \tag{1}$$

where v_0 is a constant and v the ion velocity perpendicular to the surface; this assumes single binary collisions for the scattered He^+. The results we reported recently[1] clearly show that such a neutralization model is insufficient. In this paper we will discuss the comparison between experimental data and computer simulation of the scattering process in more detail, especially the dependence of the backscattering on the crystallographic orientation.

II. THE SIMULATION MODEL

ARGUS , the computer code used for the calculation, was designed specifically for ion scattering in the near surface region. Our aims are (a) to match the experimental situation as closely as possible in the generation of the angle-resolved energy spectra of the backscattered particles, (b) to provide a method of distinguishing the trajectory-types comprising these spectra, and (c) to achieve the computation speeds necessary to obtain statistically meaningful spectra, particularly for light particle beams such as He^+ to which the surface region appears very transparent.

ARGUS is based on the binary-collision approximation in which the particle paths are traced by ordered sequences of isolated binary encounters with the solid atoms. The model is fully three dimensional (3D) and allows extensive options for the near surface lattice configuration, i.e., surface arrays and plane types, absorbed atoms, vacancies, initial impact areas, etc. The search procedure, to find the next collision partner for a moving ion, is confined where possible to a fixed subset of the solid atoms, thus avoiding geometrical continuation of the lattice. The thermal properties of the solid atoms may be simulated in a rather general manner, including nonisotropic vibrations in three dimensions, differences in thermal properties between surface and subsurface layers, and equal-time correlations.

The classical dynamics of the binary collisions are described in the center-of-mass system and moderated by a given interatomic potential function; the choices for the latter in ARGUS include the Bohr, Born-Mayer, and Thomas-Fermi-Molière potentials.[10] The collision problem is solved by one of a combination of methods: (a) Since the initial ion-atom encounter always occurs at the same initial energy with only the impact parameter being changed, table lookup is used for the first collisions; (b) the momentum approximation for binary collisions[11] is used in its ranges of validity using a rapid table lookup method; (c) when method (b) is not applicable a combination of spline and Lagrangian interpolation is used in precalculated tables; and (d) in the relatively rare cases ($\sim 3\%$) where none of the foregoing is possible, the full Gauss-Mehler[12,13] integration method is employed to solve the collision problem. A more detailed discussion of the above scheme has been given elsewhere[14] ; its net effect is to substantially reduce the time needed for the solution of the binary-collision event. In the calculations reported here the "time integral"is also computed (but not, of course, in the case of the momentum approximation) and used to offset the trajectory of the particle after the collision. Inelastic (electronic) energy losses are included in the program but not in the present calculations—not only are they small for the low energies considered here but also no reliable theory of electronic stopping is available for the sub-keV energy region.[4,15]

Particular attention has been given in the program to simulating realistic particle detectors by means of circular aperture fixed-solid-angle collectors. Each such "detector" consists of a set of identical subdetectors designed to "see" only particles with a specified class of trajectory history, thus allowing one to study how the total spectrum obtained is composed of these classes. Energy resolution effects in the detectors are included by representing each detected particle as a Gaussian pulse of width typical of the experimental detector's energy resolution, spread over several "channels" of the detector and centered at the particle's nominal backscattered energy.

For each simulation run, typically 10^6 impinging ions, details of the backscattered particles are stored on a mass storage medium. Thus further processing such as changes in detector location, energy or angular resolution, particle classifications, time histories, etc., can be affected with little additional computation. Hence ARGUS is a very high-speed computer code for ion scattering with substantial generality and flexibility.

III. EXPERIMENT

A complete discussion of the experimental system used has been published elsewhere[16] and only a brief summary is necessary here. The experimental data were obtained in a UHV system which allows the determination of ion backscattering intensities with respect to energy and laboratory scattering angle. The target cleanliness was monitored by ion scattering and Auger-electron spectroscopy; the target crystal lattice periodicity was inspected by low-energy electron diffraction (LEED). The target was mounted on a manipulator providing two axes of rotation, which define the impact angle relative to the surface and the azimuthal angle ϕ relative to a crystallographic orientation.

In the experiments described here, we used a Ni single crystal cut and oriented to better than 0.5° to the surface normal direction. The crystal was mechanically polished and electropolished. It was

then sputtercleaned and annealed *in situ* until no traces of impurities (mainly O, C, and segregated S)could be detected and a clean (1×1)—LEED pattern was observed. The measurements with a 600-eV $^4He^+$ beam of 1×10^{-8} Å caused no detectable damage of the surface. The $^4He^+$ beam was magnetically analyzed and collimated to $\pm2°$. The analyzer was a spherical 90° electrostatic prism with an energy resolution of 2% and an angular acceptance of $\pm2.5°$. The ions were detected with a channeltron and pulse counting methods used to process the output. (No neutrals could be detected with the system.) All measurements were done at room temperature.

IV. RESULTS

Figure 1 shows comparisons between the experimental and calculated spectra for 600-eV He^+ incident on a Ni(110) surface. The beam angle of incidence is 60° from the surface normal and the total scattering angle is 60°, i.e., the detector is also 60° form the surface normal. (The same geometry can also be expressed as $\psi=30°$, $\theta=60°$; see, e.g., Refs. 4 and 17.) The azimuthal angle of the beam ϕ, is defined with respect to the [110] axis in the surface, i.e., $\phi = 0°$ indicates that the incident beam and the detector are in a plane perpendicular to the crystal surface and containing the surface [110] axis $\phi=90°$ indicates the plane containing the surface [100] axis. Figure 1 shows that whereas the experimental results show little or no dependence on azimuthal angle, the calculations predict a marked azimuthal dependence and one which varies for three choices of interatomic potential. The potentials used are (i) a Born-Mayer (BM) potential $V(r) = C_{BM}\exp(-r/a_{BM})$ with $C_{BM} = 1762.7$ eV and $a_{BM} = 0.025\,839$ nm according to Abrahamson,[18] (ii) a Thomas-Fermi-Molière (TFM) potential $V(r) = (C_{TF}a_F/r)\Phi(r/a_F)$ with $C_{TF} = 6538.36$ eV and $a_F = 0.013\,74$ nm according to Firsov[19] and with Molière's screening function $\Phi(r/a_F)$,[20] and (iii) a Thomas-Fermi-Molière potential (0.8 TFM) with a Firsov screening length reduced by a factor 0.8, which is suggested by some experimental results.[4,21] Furthermore the TFM potential for helium-nickel derived with assumptions (iii) is in close agreement with the potential calculated by Wilson *et al.*[22] In Fig. 1 the calculated spectra have been normalized so that the largest calculated peak approximately corresponds to the experimental one.

Figure 2 summarizes the experimental results. One can see that the peak location, height, and width are very weakly, if at all, dependent on ϕ. This fundamental discrepancy between the calculations and the experiments thus raises the possibility that some form of trajectory-dependent neutralization could be present.[1]

In order to further explore this possibility, the

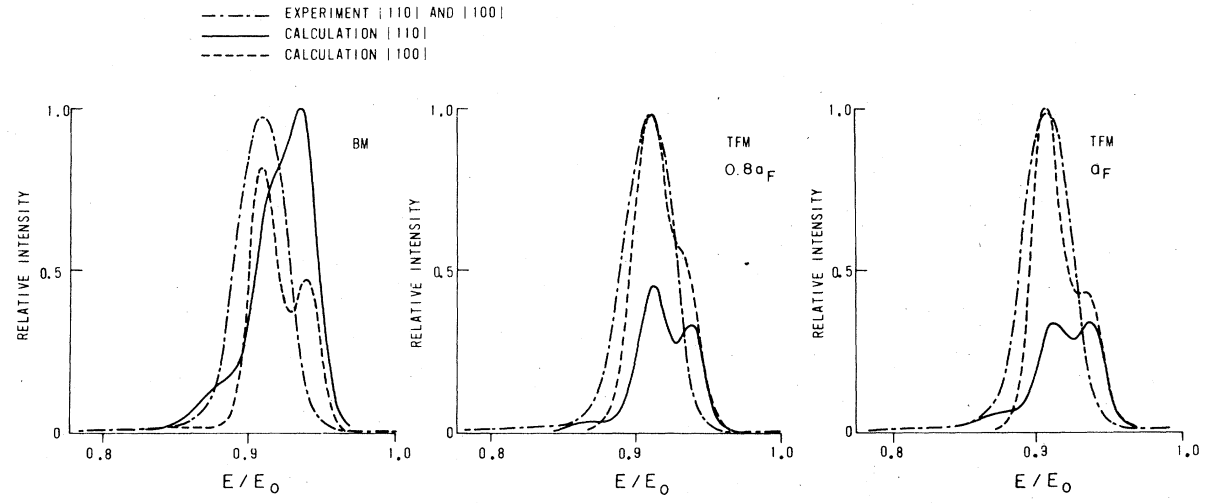

FIG. 1. Comparison of the experimental (—·—·—) and calculated results from ARGUS for 600-eV He^+ ions incident at 60° to the surface normal. The ARGUS calculations for the azimuthal angles $\phi=0°$ (—) and $\phi=90°$ (----) are shown for three choices of the ion-atom interatomic potential function: (i) BM—Born-Mayer, (ii) TFM $(0.8a_F)$= Thomas-Fermi-Molière with 0.8 times the Firsov screening radius, and (iii) TFM (a_F) = Thomas-Fermi-Molière with the usual Firsov screening radius (a_F).

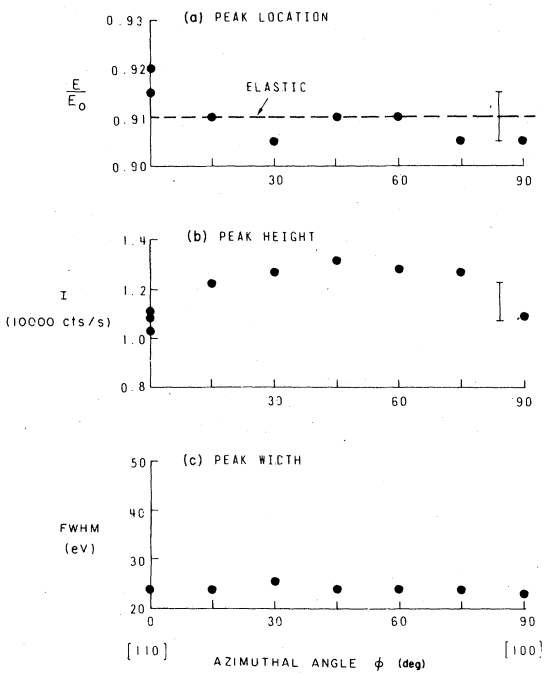

FIG. 2. A summary of the experimental results plotted as a function of azimuthal angle ϕ: (a) the peak location where E_0 = incident beam energy, (b) the peak height, and (c) the peak width where FWHM = full width at half maximum.

reflected particles obtained in the calculations were sorted according to their class—i.e., on the basis of trajectory type. In Figs. 3 and 4 the total reflected intensity is shown to be composed of distinct classes which exhibit significantly different dependences on the beam crystallographic orientation. Figure 4 has been drawn with the total peak at 0.95 for each case in order to show components clearly; the absolute magnitude can be seen in Fig. 3. The only class showing no angular dependence is "single I," which contains trajectories formed by one violent collision leading approximately to the detector scattering angle of 60°. Additional small deflections of less than 5° may also be present. These trajectories are further restricted to interactions with the top monolayer of the surface. "Single II" is defined as a violent collision occurring with the second layer only. Such trajectories are only possible close to the [110] ($\phi=0°$) and [100] ($\phi=90°$) surface half channels; from $\phi=30°$ to $\phi=75°$ the second layer is effectively blocked by the top layer. In the latter range single I provides up to 60% of the total intensity, which gives some credibility to the use of the single binary scattering model widely used for surface analysis,[17] i.e., single scattering may well dominate in the case of polycrystalline surfaces.

The "string-I" and "string-II" components are defined as due to trajectories which involve two or more collisions with atoms belonging to the same atomic string of surface atoms, each leading to a deflection greater than 5°. I and II refer to the top and second layers as above. The string components contribute only for directions close to the two major channels, where they contribute 18% [110] and 3% [100] to the total intensity. This is an obvious example where the use of chain or string models[2] alone would be very misleading, even when using a 2D detector, and the results would be even worse for a model which included only in-plane scattering.

Unlike chain or string models which would only include the classes defined previously, the current 3D calculations demonstrate the occurence of two other classes denoted here as "zig zag I" and "zig zag II." The former includes trajectories with multiple interactions only, with the first surface layer in conformity with our previous convention; however, unlike the "string classes", these particles do not follow a principal surface direction in a systematic manner. They can be visualized as random-walk-like processes with the restriction that reversal of forward momentum is unlikely. Zig zag I adds to the total intensity over the whole azimuthal range and is of the same order of magnitude as single I. In Fig. 3, it can be seen that this zig zag class contributes up to 30% of the total intensity in the region of the intensity minimum. However, Fig. 4 shows that this contribution is mainly in the high-energy peak whereas the lower energy "single" peak is mainly (90%) due to class single I. Thus out-of-plane scattering on the surface with zig-zag-type patterns is a relatively common trajectory type.

For zig zag II the random-walk pattern must be understood as fully 3D. It also includes those particles which make collisions with first-layer atoms preceded or followed by second-layer collisions; thus it includes the interlayer component of the scattering. The class zig zag II forms maxima when the plane of scattering is aligned parallel to the [100] surface rows, or along [110] and even when slightly off the latter direction. This may be understood as a flux focusing effect slightly modified by transparency effects. The transparency variation can be judged from the relatively smooth variation of the total reflection coefficient with azimuthal angle as compared to that of the doubly

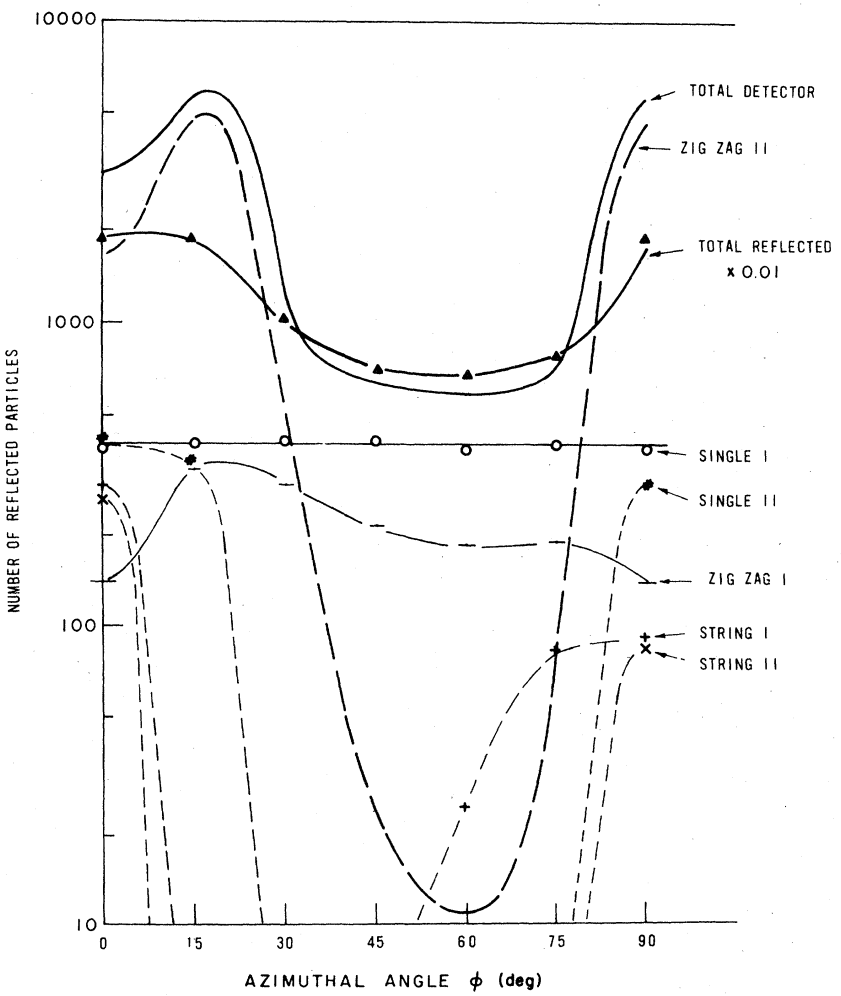

FIG. 3. The dependence of the appearance of calculated trajectory classes on azimuthal angle ϕ (0.8 TFM). The symbols are as follows: (—) total in the angle-resolved detector, (- -) total particles reflected into the hemisphere (+) "string I," (×) "string II," (—) "zig zag I," "single I," (o) "string II," (----) "zig zag II".

differentiated detector intensity (Fig. 3). The zig zag II class becomes practically negligible in the region of the minimum due to the blocking of the second layer by the first layer as do string II and single II. Figure 5 helps to make the particle classifications somewhat clearer. The single and stringlike trajectories denoted by "×" on the graph behave in the manner expected from string models.[2] They form the usual "loop", e.g., energy versus scattering-angle pattern, expected for multiple scattering and also of course the single classes fall on the curve calculated from elementary elastic scattering considerations. The zig zag particles denoted by (●) appear in the two roles: (a) as a background (mainly forward scattered) to the well-defined 2D classes of particles and (b) involved in the multiple-scattering region for interlayer scattering events, in many cases introducing perturbations in the loop not normally seen in chain-type models.

Table I demonstrates the influence of the potential parameter on the calculated spectra. For the two "extreme" directions chosen, the contribution of the zig-zag collisions is extremely large. As can be seen from the table, this contribution can vary by much as an order of magnitude, e.g., for the [110] direction, whereas the single-scattering contribution changes by only a factor of 2 when going from BM to 0.8 TFM. In relative numbers the stringlike classes and zig zag I do not change. Zig zag II is reduced by a factor of 2 and the singles increased by a factor of 2. For the [100] direction the changes in absolute number are largest for

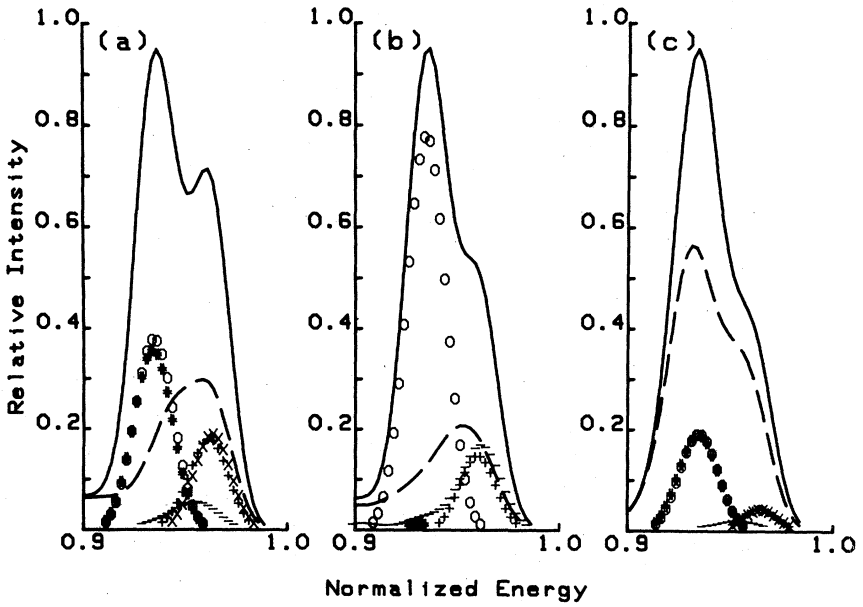

FIG. 4. The energy spectra for particles as calculated for a detector located at a scattering angle of 60° form the incident beam (0.8 TFM). The symbols for the classes are as in the caption to Fig. 3. Note that the "zig-zag I" class is represented by dashes (-) and the "zig-zag II" class by the broken line. The distributions are shown for (*a*) $\phi=0°$, (*b*) $\phi=75°$, and (*c*) $\phi=90°$.

the stringlike classes and the zig zag I, whereas zig zag II decreases only by a factor of 2. The relative changes are again a factor of 2 up for the singles, but no great changes occur for zig zag II, and the remainder decrease to very low levels. This reflects the difference in the structure of the [100] and [110] surface channels which obviously have a very strong influence on the more complex

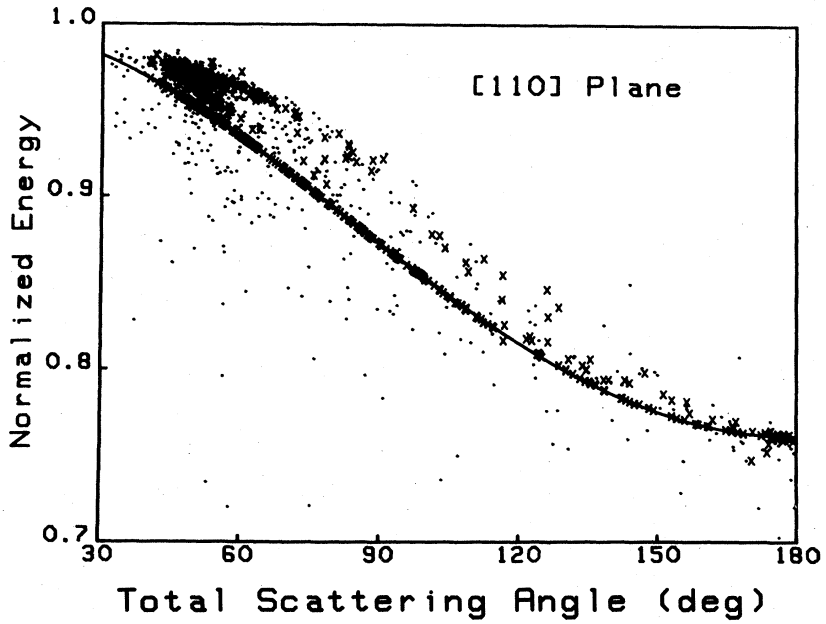

FIG. 5. A plot of backscattered energy versus total scattering angle calculated for the reflected particles (potential 0.8 TFM). The solid line is the single collision curve and the classes are denoted: (●) for "zig zag I" and "zig zag II" and (×) for all other classes.

trajectories. These channels cause small-angle collisions which are most sensitive to the form of the potential and are also decisive for the blocking and focusing effects observed here.

V. DISCUSSION

It is unlikely that the discrepancy between the experiments and the calculations can be ascribed to intrinsic errors in either. The experimental results have shown reproducibility to better than 10% for differently prepared Ni(110) surfaces at different times (1972 to 1979). Also, other laboratories working with this, other Ni, and comparable Cu surfaces have not reported any azimuthal dependences[8,21,23] due to multiple collisions similar to those calculated here for reflected ions. In Ref. 1 excellent agreement between experiment and ARGUS calculations (0.8 TFM interatomic potential) was obtained for Li^+ ions on the same surface for a case where trajectory-dependent neutralization was not significant. This indicates the validity of the ARGUS calculations and reinforces our choice of interatomic potential although the latter is not critical to the arguments that follow. Furthermore the total reflection coefficients for backscattering predicted by ARGUS can be reproduced using the computer code MARLOWE,[5] thus providing an independent check on the calculations. Hence we infer that the differences between the experiments and the calculations are due to neutralization effects and the remainder of this discussion will proceed on that basis. Experimental results indicate that $v_0 = 3.7 \times 10^7$ cm s^{-1} (Ref. 8), $v_0 = 2.88 \times 10^7$ cm s^{-1} (Ref. 9), or $v_0 = 1.78 \times 10^7$ cm s^{-1} (Ref. 1) are appropriate values for Eq. (1). However it is clear that this simple neutralization model is bound to fail since using the same value of P for the "total" curves in Fig. 3 will not give the essentially constant yield versus ϕ observed in experiment (Fig. 2). In reality such a procedure can only be consistently applied to the single peak for which v_0 was evaluated in the aforementioned experiments.[1,8,9] A better approach can be based on the observation that the neutralization for He scattered from Ni at somewhat higher beam energies ($\gtrsim$ 1.5 keV) is due to different processes for surface and "bulk" scattered particles.[24] In the latter experiments the ion fraction as a function of secondary energy shows a surface peak, i.e., particles not scattered from the surface are more effectively neutralized. The remainder of the particles are mostly backscattered from deeper bulk layers, appearing in the spectrum at energies below the surface peak. In the present work we have to deal mainly with particles scattered into higher energies and from the second layer at most. For the particles scattered from the bulk the experimental charge-state fraction $f^+ = n^+/(n^0+n^+)$ (where n^+ is the number of reflected ions and n^0 the

TABLE I. Particle yields for He on Ni(100) at (60° in, 60° out) and 600 eV for 3×10^6 incident He ions.

Potential	String		Zig zag		Single		Detector	Reflected
	I	II	I	II	I	II	total	total
			(a) The plane of scattering parallel to [110] $\phi = 0°$					
BM	2378	2323	1085	16888	1584	1583	25841	850909
TFM	857	778	440	4711	1171	1151	9114	538089
0.8 TFM	414	395	191	1531	933	959	4423	331867
			Normalized to detector total					
BM	0.0920	0.899	0.0419	0.654	0.0613	0.0612	1.00	
TFM	0.0940	0.854	0.0483	0.517	0.128	0.126	1.00	
0.8 TFM	0.0936	0.893	0.0432	0.346	0.211	0.216	1.00	
			(b) The plane of scattering parallel to [100] $\phi = 90°$					
Bm	825	565	1096	11878	1638	1025	17026	679212
TFM	326	272	424	14013	1170	943	17148	579227
0.8 TFM	181	153	210	6121	906	945	8516	391407
			Normalized to detector total					
BM	0.0484	0.0332	0.0644	0.698	0.0962	0.0602	1.00	
TFM	0.0190	0.0160	0.0247	0.817	0.0682	0.0550	1.00	
0.8 TFM	0.0212	0.0180	0.0246	0.718	0.016	0.111	1.00	

number reflected as neutrals) is a linear function of the energy, i.e., $f^+ \propto E$.[24] The measurements were taken above 2 keV (Ref.24) and extrapolation down to 600 eV would give a value of $f^+ \approx 10^{-3}$ for He^+ scattered from the bulk. In the present calculations this value would reduce the zig zag II down to the percent level of the single I and all the remainder down to the experimental noise level. The result of such a neutralization model is shown in Fig. 6. The single I intensity has been reduced by 10^{-3}, and the new total was obtained by summation. The result is still weakly dependent on the azimuthal angle, but now more compatible with the experimental data (Fig. 2).

The procedure leading to Fig. 6 is based on the assumption that the ions scattered from the second layer or following extended trajectories across the surface are subject to a neutralization process, which is comparable to the neutralization process of particles scattered through the bulk. Tentative models for the "bulk neutralization" involve a steady-state situation in which the ion travels within a cloud of electrons. This situation has been described as an equilibrium between capture and loss processes[25] or as dynamic screening effect.[26] With respect to the present calculations, both models raise two questions, i.e., is the time scale adequate for an adoption of these models for surface multiple scattering and is the electron density sufficiently bulklike? The time scales involved

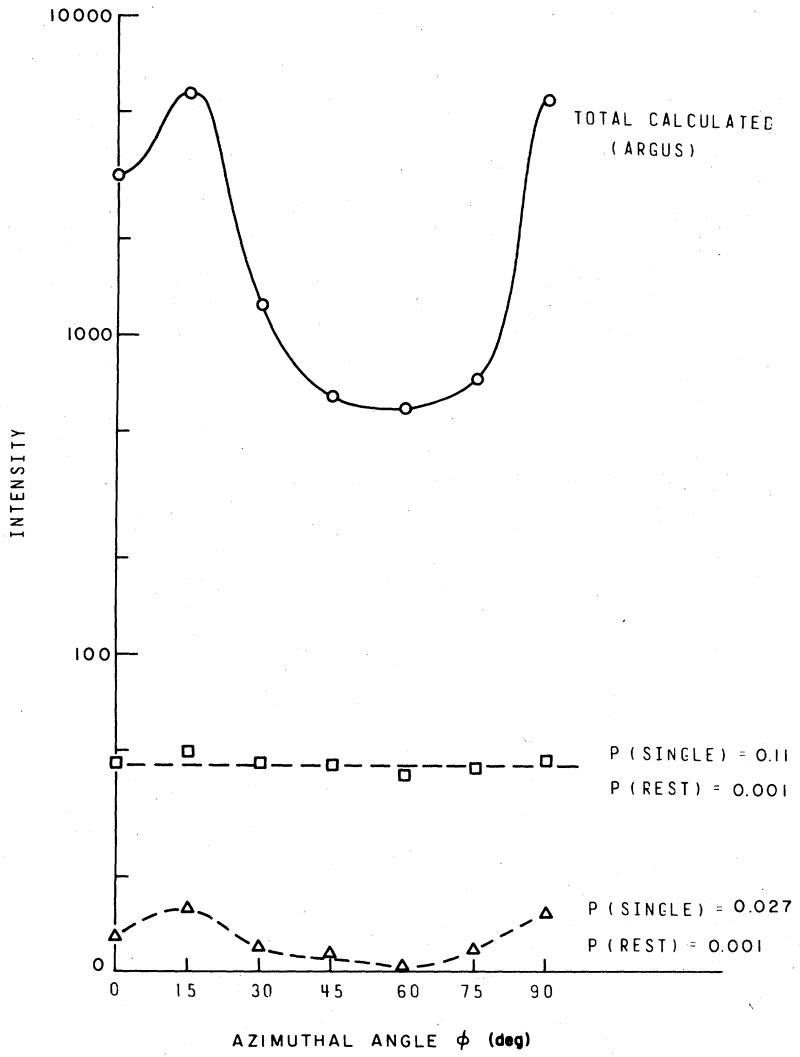

Fig. 6. The effect of applying the indicated neutralization models to the calculated results as a function of azimuthal angle. Lines are drawn to guide the eye.

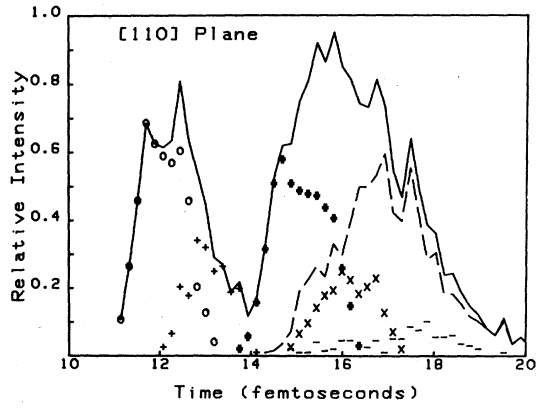

FIG. 7. The calculated time distributions of the various trajectory classes for $\phi=0°$ azimuthal beam angle (0.8 TFM). The symbols are as defined in the caption to Fig. 3.

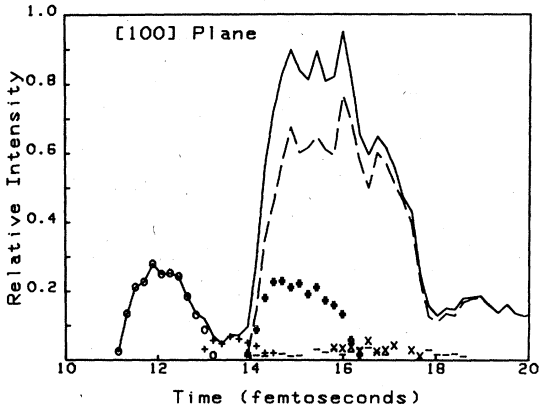

FIG. 8. The calculated time distributions of the various trajectory classes for $\phi=90°$ azimuthal beam angle (0.8 TFM). The symbols are as defined in the caption to Fig. 3.

in the surface scattering events are shown in Figs. 7 and 8 as evaluated with ARGUS. In order to obtain a time origin for the simulation model some assumption must be made concerning the height above the surface at which a particle no longer experiences any influence of the solid. In the present calculations we have arbitrarily assumed that this height is 1.5 lattice spacings for Ni (i.e., 0.532 nm)— this simply sets the origin of the time scale given in Figs. 7 and 8 and does not affect the scale or the absolute differences between the times of the trajectory classes. For the present height assumption a He^+ ion incident 60° to the surface normal which penetrates to the geometrical surface plane and is there reflected with 60° total scattering angle into the center of the detector, would have a time of 12.4 fs. In fact, as seen in Figs. 7 and 8, this time can be somewhat less for single I since the atoms project above the nominal geometric surface plane and because of the finite spatial resolution of the detectors. The really striking feature of the curves is their double-peaked shape indicating the presence of two time groups with a distinct minimum in the time envelope near 13.5—14 fs. For the $\phi=0°$ case (Fig. 7) the first peak contains the single I class and essentially all of the string I particles—the latter group contributing about 31% of the first peak height. The $\phi=90°$ case (Fig. 8) shows that 95% of the first peak is due to single I particles. Since the experimental evidence for He scattering shows no high-energy peaks or shoulders, this would exclude string I and zig zag I, and the lack of observed azimuthal dependence would exclude single II from the observed spectra. Furthermore zig zag II, and string II ions would clearly be neutralized under any model which hypothesized the neutralization of the aforementioned groups. Thus it is apparent that our previous assumptions of distinct surface and bulk neutralization processes would be made largely plausible by assuming the onset of bulk neutralization processes at somewhat less than 13.5—14.0 fs. At present the "time" frame for the different neutralization processes cannot be more precisely stated. However the present work clearly demonstrates the significance of trajectory dependence effects and provides a theoretical framework in which the hitherto confused topic of neutralization can be approached.

VI. CONCLUSIONS

The major results presented here may be summarized as follows.

(a) A three-dimensional model with high numbers of detected particles is required to understand the details of ion scattering; chain and string models give grossly misleading information on backscattered particle intensities.

(b) The neutralization process is strongly dependent on the trajectory of the scattered particle for the cases studied here.

(c) At least two distinct types of neutralization phenomena are present; one essentially Auger and the other more typical of the bulk effects seen at higher energies.

ACKNOWLEDGMENTS

One of us (W. H.) is indebted to S. Datz, M. T. Robinson, and O. S. Oen for helpful discussions.

[1]E. Taglauer, W. Englert, W. Heiland, and D. P. Jackson, Phys. Rev. Lett. 45, 740 (1980).
[2]For reviews, see E. S. Maskhova and V. A. Molchanov, Radiat. Eff. 23, 215 (1975); 16, 143 (1972); W. Heiland and E. Taglauer, Nucl. Instrum. Methods 132, 535 (1976).
[3]E. S. Parilis, N. Yu. Turaev, and V. M. Kivilis, *Proceedings of the 7th International Conference on Phenomena in Ionized Gases, Belgrade, 1965,* edited by B. Perovic and D.Tosić (Gradjevinska Knjiga, Belgrade, 1966), p. 47.
[4]W. Heiland, E. Taglauer, and M. T. Robinson, Nucl. Instrum. Methods 132, 655 (1976).
[5]M. T. Robinson and I. M. Torrens, Phys. Rev. 93, 5008 (1974).
[6]B. J. Garrison, Surf. Sci. 87, 683 (1979).
[7]*Inelastic Ion Surface Collisions,* edited by N. H. Tolk, J. C. Tully, W. Heiland, and C. W. White (Academic, New York, 1977).
[8]H. H. Brongersma and T. M. Buck, Nucl. Instrum. Methods 132, 559 (1976).
[9]W. Englert, W. Heiland, E. Taglauer, and D. Menzel, Surf. Sci. 83, 243 (1979).
[10]I. M. Torrens, *Interatomic Potentials* (Academic, New York, 1972).
[11]C. Lehmann and G. Leibfried, Z. Phys. 172, 465 (1963).
[12]F. J. Smith, Physica 30, 497 (1964).
[13]M. T. Robinson, ORNL-4556 (unpublished).
[14]D. P. Jackson, J. Nucl. Mater. 93/94, 507 (1980).
[15]W. Heiland and E. Taglauer, in Ref. 7.
[16]E. Taglauer, W. Melchior, F. Schuster, and W. Heiland, J. Phys. E 8, 759 (1975).
[17]E. Taglauer and W. Heiland, Appl. Phys. 13, 47 (1977).
[18]A. A. Abrahamson, Phys. Rev. 179, 766 (1969).
[19]O. B. Firsov, Zh. Eksp. Teor. Fiz. 33, 696 (1957) [Sov. Phys.—JETP 36, 1076 (1959)].
[20]G. Molière, Z. Naturforsch. 29, 133 (1947).
[21]B. Poelsema, L. K. Verhey, and A. L. Boers, Surf. Sci. 64, 554 (1977).
[22]W. D. Wilson, L. G. Haggmark, and J. P. Biersack, Phys. Rev. B 15, 2458 (1977).
[23]T. M. Buck (private communication).
[24]W. Eckstein, V. A. Molchanov, and H. Verbeek, Nucl. Instrum. Methods 149, 599 (1978).
[25]E. S. Parilis, *Proceedings of the 7th International Conference on Atomic Collisions in Solids, Moscow, 1977* (in press).
[26]J. Zwiegel, thesis, München, 1979 (unpublished).